Structural Examination of Enantioselective Intercalation: ^{1}H NMR of Rh(en)$_2$phi^{3+} Isomers Bound to d(GTGCAC)$_2$[†]

Thomas P. Shields and Jacqueline K. Barton*

Division of Chemistry and Chemical Engineering, California Institute of Technology, Pasadena, California 91125

Received June 13, 1995; Revised Manuscript Received August 25, 1995[⊗]

ABSTRACT: The enantioselective recognition of d(GTGCAC)$_2$ by Δ- and Λ-Rh(en)$_2$phi^{3+} (en = ethylenediamine; phi = 9,10-phenanthrenequinone diimine) has been examined in a series of one-dimensional (1D) and two-dimensional (2D) 500 MHz ^{1}H NMR experiments both to extend our understanding of the basis for the enantioselective DNA binding and to gain structural information concerning intercalation by the octahedral metal complexes. Δ-Rh(en)$_2$phi^{3+} forms a symmetric 1:1 complex with d(GTGCAC)$_2$, and the metal complex is in slow exchange with the oligodeoxynucleotide bound form at 295 K. The strong upfield shifts of the phi ligand's aromatic protons (0.6−1.3 ppm) are consistent with full intercalation of the phi ligand into the DNA base stack. 2D-NOESY experiments reveal a loss in internucleotide connectivity between G_3 and C_4 bases, while new NOE cross peaks are observed between the phi ligand and the G_3 deoxyribose sugar. In contrast to binding by Δ-Rh(en)$_2$phi^{3+}, the 1:1 Λ-Rh(en)$_2$phi^{3+}−d(GTGCAC)$_2$ complex shows much broader resonances, and both metal complex and DNA protons appear to be in the intermediate exchange regime. The loss of C_2 symmetry in the 1:1 complex is consistent with binding by Λ-Rh(en)$_2$phi^{3+} at the T_2G_3 step. Although the enantiomeric metal complexes display different sequence selectivities and exchange characteristics, Λ- and Δ-Rh(en)$_2$phi^{3+} interact with the oligonucleotide duplex in a fundamentally similar manner, through the full intercalation of the phi ligand. Upfield movements in chemical shifts of phi protons are nearly identical for the two enantiomers, and both Λ- and Δ-Rh(en)$_2$phi^{3+} stabilize the duplex to melting by 5−10 °C. Given the common binding mode of the two enantiomers, the differences in their binding characteristics emanate from interactions with the ancillary nonintercalating ligands. Thus, as a general strategy, intercalation may provide an anchor for sequence-selective interactions of octahedral metal complexes in the groove of duplex DNA.

Our laboratory has focused on the design of octahedral complexes for the sequence-selective recognition of duplex DNA (Dupureur & Barton, 1995). The octahedral geometry of transition metal complexes may be exploited in anchoring a chelated intercalating ligand in the major groove of DNA and, in so doing, orienting nonintercalating ligands of the octahedral complex in the helical groove for sequence-selective interaction. Perhaps the simplest example of this strategy for recognition is visible in the structures of Λ- and Δ-Rh(en)$_2$phi^{3+} (Figure 1). Both isomers contain the extended aromatic phi ligand for intercalative stacking in the DNA duplex as well as axial amines for potential hydrogen bonding in the groove; the isomers differ with respect to the disposition of their ancillary ethylenediamine ligands.

Biophysical studies indicate that these enantiomers bind tightly to DNA via intercalation of the planar aromatic phi ligand (Krotz et al., 1993a,b; Shields & Barton, 1995). For Δ-Rh(en)$_2$phi^{3+}, DNA site affinities range from 0.3 to 8.0 × 10^6 M^{-1}, and a distinct preference for GC sites is evident. Λ-Rh(en)$_2$phi^{3+} is found to be sequence neutral with site selectivities of 2 × 10^6 M^{-1}. These differences in site recognition between enantiomers have been attributed to the different hydrogen bonding and van der Waals contacts available in the major groove with the ancillary ethylenediamine ligands of the two isomers. The range of recognition elements, hydrogen bonding, and van der Waals contacts, as well as shape selection, may be assembled together using the octahedral framework of Rh(phi)$^{3+}$ intercalators to create an array of complexes designed rationally for sequence-specific DNA binding. Indeed, by using Rh(en)$_2$phi^{3+} as a starting point, Δ-α-[Rh-(R,R)-Me$_2$(trien)phi]$^{3+}$ has been constructed and demonstrated to target the sequence 5′-TGCA-3′ based upon an ensemble of sequence-specific noncovalent contacts (Krotz et al., 1993a,b; Hudson et al., 1995).

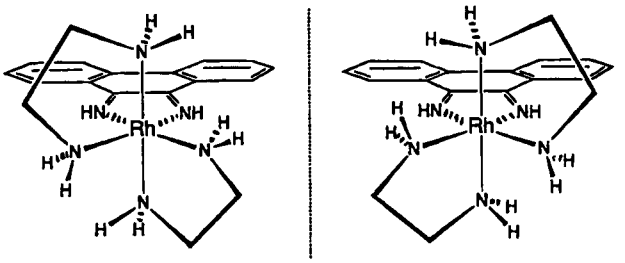

FIGURE 1: Structures of Λ-Rh(phen)$_2$phi^{3+} (left) and Δ-Rh(en)$_2$-phi^{3+} (right).

Such rational design requires a detailed structural understanding of the metal complex bound to its DNA recognition site. Moreover, in developing a general strategy of DNA recognition based upon the systematic variation of functional groups and functional group placement on the ancillary

[†] Supported by grants to J.K.B. from the National Institutes of Health (GM33309) and an NIH-NRSA predoctoral fellowship to T.P.S.

* Author to whom correspondence should be addressed.

[⊗] Abstract published in *Advance ACS Abstracts,* November 1, 1995.

0006-2960/95/0434-15049$09.00/0

ligands of the octahedral intercalator, it becomes important to compare and contrast binding modes and orientations for different complexes. Early NMR studies of tris(phenanthroline) metal complexes bound to oligonucleotides showed that the complexes bound DNA with fast exchange kinetics. Both enantiomers were shown to bind similarly through two binding modes, partial intercalation in the major groove and hydrophobic association against the minor groove; the major groove intercalation favored the Δ-isomer, and the minor groove association favored the Λ-isomer (Rehmann & Barton, 1990a,b). Later 2D-NMR studies focused on the minor groove binding mode (Eriksson et al., 1994). 2D-NMR experiments with Δ-$Rh(phen)_2phi^{3+}$ established directly a site-specific intercalation by the octahedral metal complex with the partial insertion of the phi ligand between the central 5′-CG-3′ step of the oligomer 5′-$d(GTCGAC)_2$; several intermolecular NOE contacts also supported a major groove orientation for the rhodium intercalator (David & Barton, 1993).

NMR data for $Rh(NH_3)_4phi^{3+}$ bound to $d(TGGCCA)_2$ confirmed that the smaller $Rh(NH_3)_4phi^{3+}$ binds to DNA through classical intercalation (Collins et al., 1994). For the series $Ru(phen)_3^{2+}$, $Rh(phen)_2phi^{3+}$, and $Rh(NH_3)_4phi^{3+}$, an increased depth of intercalation is evident, as is a decrease in exchange rate. For $Rh(NH_3)_4phi^{3+}$, the complete insertion of the phi ligand into the aromatic DNA base stack orients the axial ammine ligands for hydrogen bonding to the guanine O6 atoms of the central 5′-GC-3′ step. A high-resolution structural model of Δ-α-[Rh-(R,R)-Me_2(trien)-phi]$^{3+}$ bound site specifically to its target 5′-TGCA-3′ within a DNA decamer has recently been developed using two-dimensional NMR methods (Hudson et al., 1995), and this structure reveals intercalation into the central 5′-GC-3′ step from the major groove with specific methyl−methyl contacts between the ancillary Me_2(trien) ligand and 5′-thymines above and below the intercalated GC base step.

Here, using ^{1}H NMR spectroscopy, we compare structural parameters for Λ- and Δ-$Rh(en)_2phi^{3+}$ bound to duplex DNA. We find that both enantiomers bind to the duplex tightly through a similar intercalative mode characterized by the complete insertion of the aromatic phi ligand between DNA base pairs. The differences in site selectivity between these enantiomers can be understood on the basis of the differing stereochemistry of the ancillary ligands in the two isomers and the abilities of these nonintercalating ligands to interact noncovalently in the DNA major groove.

EXPERIMENTAL PROCEDURES

Materials. Enantiomers of $Rh(en)_2phi^{3+}$ were prepared as previously described (Schaefer et al., 1992; Krotz et al., 1993a,b), and metal concentrations were quantitated by UV−visible spectroscopy. The self-complementary deoxyoligonucleotide $d(GTGCAC)_2$ was synthesized on an ABI Model 392 DNA synthesizer using phosphoramidite chemistry, purified by reverse-phase HPLC and FPLC, and quantitated with an extinction coefficient of 6600 M^{-1} cm^{-1} per nucleotide at 260 nm.

Instrumentation. UV−visible spectra were measured on either a Hewlett-Packard 8452A diode array spectrophotometer or a Cary 2200 spectrometer. High-performance liquid chromatography (HPLC) was performed with a Waters 600/600E multisolvent delivery system equipped with a Waters 484 tunable wavelength detector and a VYDAC protein and peptide C18 column. FPLC was performed on a Pharmacia FPLC system equipped with an LCC-500 plus controller, an LKB 2141 variable wavelength detector, and a PepRC 15 μM HR 16/10 (C18) column.

NMR Experiments. NMR spectra were obtained in 99.96% D_2O (Cambridge Scientific), and all samples were in phosphate buffer (10 mM NaH_2PO_4/Na_2HPO_4, 20 mM NaCl, pH 7.0). DNA samples were dissolved in 0.5 mL of phosphate buffer, repeatedly lyophilized from 99.8% D_2O, and then finally resuspended in 99.96% D_2O. Aliquots of a concentrated stock solution of Λ- or Δ-$Rh(en)_2phi^{3+}$ were titrated directly into the NMR tube. Stoichiometric ratios were determined using UV−visible spectroscopy.

^{1}H NMR spectra were recorded on a Bruker AMX-500 spectrometer operating at 500 MHz. Chemical shifts are referenced to sodium 3-(trimethylsilyl)-1-propanesulfonate (TSP) at the corresponding temperature. The two-dimensional (2D) COSY and NOESY experiments were acquired in the phase-sensitive mode using the time-proportional phase incrementation method (Marion & Wuthrich, 1983). The spectra were recorded with the carrier frequency placed on the HDO resonance using 2048 points in t_2 for 512 t_1 values and a pulse repetition rate of 1.6 s. NOESY spectra were acquired for mixing time values of 200 and 300 ms. A presaturation pulse was utilized to suppress the HDO resonance. One-dimensional (1D) and 2D-NMR spectra were processed with the FELIX software package (Biosym Technologies, San Diego, CA). 1D-NMR spectra were apodized with a simple exponential multiplication (1 Hz line broadening) prior to Fourier transformation, while 2D-NMR spectra were apodized with a shifted sine bell or a squared sine bell, zero filled twice in t_1, and Fourier-transformed in both dimensions. Variable temperature NMR experiments were carried out with a Eurotherm temperature controller.

Molecular Modeling. Molecular modeling was performed on a Silicon Graphics Iris Indigo workstation using the Biosym modeling package (Biosym Technologies, San Diego, CA). The coordinates of $Rh(en)_2phi^{3+}$ were obtained from the crystal structure (Schaefer et al., 1992). Models of $d(GTGCAC)_2$ containing intercalation sites were constructed using either the crystal structure of a dinucleotide intercalation site (Wang et al., 1978) or the Biopolymer program of the InsightII package. The DNA structures were minimized for 100 steps with a steepest descents algorithm before placing the $Rh(en)_2phi^{3+}$ enantiomer into the intercalation site.

RESULTS

^{1}H NMR of Free $d(GTGCAC)_2$. The resonances of the free hexanucleotide were assigned from NOESY and COSY spectra according to established methods (Wuthrich, 1986; Patel et al., 1986; Patel & Shapiro, 1986a,b; Liu et al., 1991) and are in agreement with results obtained at 300 MHz (Rehmann & Barton, 1990a,b). Since each base's aromatic resonance displays a stronger NOE cross peak to its own sugar H2′2″ resonances than to the sugar of the 5′-flanking residue, the oligonucleotide may be described generally by a B-type conformation (e.g., with C2′-endo sugar puckering).

1D-NMR Titration of $d(GTGCAC)_2$ with Λ- and Δ-$Rh(en)_2phi^{3+}$. The ^{1}H NMR titration of $d(GTGCAC)_2$ with Δ-$Rh(en)_2phi^{3+}$ at 295 K is presented in Figure 2. As

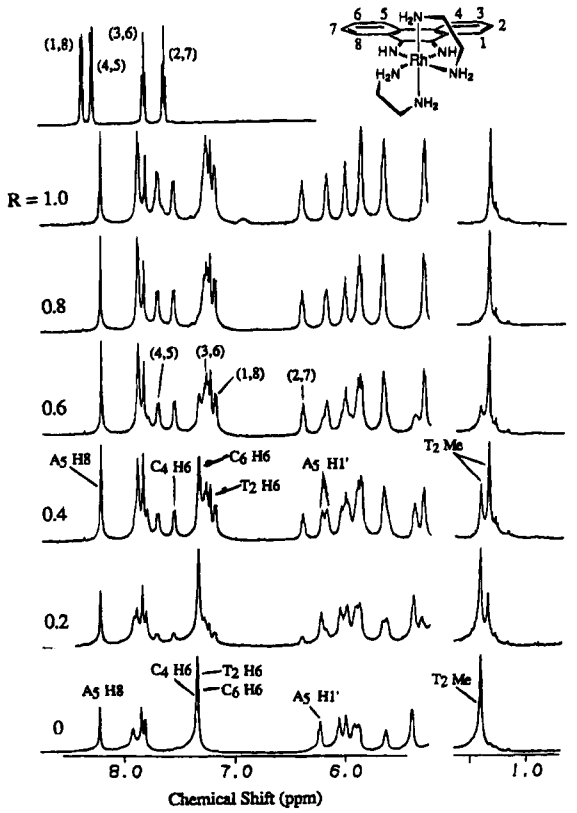

FIGURE 2: 1D-NMR titration of d(GTGCAC)$_2$ with Δ-Rh(en)$_2$phi^{3+}. 500 MHz ^{1}H NMR spectra are displayed at metal to duplex ratios of (A) 0, (B) 0.2, (C) 0.4, (D) 0.6, (E) 0.8, and (F) 1.0. The spectrum of free Rh(en)$_2$phi^{3+} under identical solution conditions is given at the top. Note that, upon addition of the metal complex, the resonances remain sharp and resolved, indicative of slow exchange. Separate free and bound resonances are observed for several protons, most notably those of C_4 H6 (7.350 and 7.564), A_5 H1′ (6.226 and 6.172), and T_2 Me (1.401 and 1.314). Also indicative of slow exchange is the growth of the phi ligand protons at a single bound chemical shift. The resonances of phi protons are given in spectra D (bound) and G (free). Both DNA and phi ligand protons retain their C_2 symmetry upon binding, which argues in support of binding at the central G_3C_4 step.

aliquots of the metal complex are added to the oligomer, the resonances of the DNA base H8/H6 and sugar H1′ protons exhibit significant changes in chemical shift (−0.04 to −0.46 ppm) but remain sharp, resolved peaks. Since the bound resonances of the C_4 H6 (7.564 ppm), A_5 H1′ (6.172 ppm), and T_2 Me (1.314 ppm) protons increase stoichiometrically with added metal complex, it is concluded that there is a single binding site for Δ-Rh(en)$_2$phi^{3+} on the oligomer. The retention of C_2 symmetry in both the DNA and phi ligand protons further argues that this binding site is the central G_3C_4 step. Since both the metal complex and the DNA retain their C_2 symmetry upon complex formation, this binding occurs without canting of the complex toward one strand within the 5′-G_3C_4-3′ binding site, a result which is consistent with the DNA photocleavage results described previously (Krotz et al., 1993a,b; Shields & Barton, 1995). Binding at the G_3C_4 step is also supported by the large changes in shifts of the C_4 H5 and C_4 H6 protons relative to the similar protons of the C_6 residue. Table 1 lists the free and bound chemical shifts of DNA base H8/H6 as well as sugar H1′, H2′, H2″, and H3′ protons.

The lack of significant broadening of the spectra upon addition of Δ-Rh(en)$_2$phi^{3+}, as well as the existence of free

Table 1: Chemical Shifts of d(GTGCAC)$_2$ Protons at 295 K[a,b]

base	H8/H6	H5/H2/Me	H1′	H2′	H2″	H3′
		(A) Free DNA Duplex				
G_1	7.842		5.98	2.65	2.80	4.81
T_2	7.335	1.40	5.92	2.22	2.55	4.90
G_3	7.875		5.87	2.64	2.73	4.98
C_4	7.350	5.40	5.63	2.05	2.39	4.81
A_5	8.220	7.92	6.23	2.67	2.87	4.98
C_6	7.316	5.33	6.05	2.11	2.11	4.46
		(B) Δ-Rh(en)$_2$phi^{3+}−d(GTGCAC)$_2$ Complex				
G_1	7.88		5.88	2.58	2.73	4.80
T_2	7.24	1.31	5.66	1.72	2.18	4.78
G_3	7.89		5.66	2.62	2.73	5.03
C_4	7.56	5.86	5.29	2.16	2.41	4.76
A_5	8.22	7.84	6.17	2.72	2.86	4.99
C_6	7.27	5.30	6.01	2.06	2.12	4.41

[a] All chemical shift data are listed in ppm and referenced to TSP at 295 K. [b] Assignments are based on a combination of 2D-NOESY and COSY spectra.

and bound resonances for several DNA protons, indicates that these protons of the metal complex are in the slow-exchange regime in binding to the oligonucleotide at 295 K. Organic intercalators typically bind to DNA with intermediate exchange kinetics (Feigon et al., 1984; Patel & Canuel, 1977; Patel & Shen, 1978; Wilson et al., 1985; Chandrasekaran et al., 1985; Delbarre et al., 1983). On the basis of the data in Figure 2, the condition of slow exchange requires that the dissociation rate of Δ-Rh(en)$_2$phi^{3+} with the duplex be significantly less than the 45 Hz chemical shift difference between the free and bound thymine methyl resonances (Wuthrich, 1986). On this basis, one may estimate an exchange rate on the order of 5 s^{-1} at 295 K for these protons, which is well within the regime of slow-exchange kinetics.

The aromatic phi protons of Δ-Rh(en)$_2$phi^{3+} were assigned on the basis of 2D-NOESY and COSY spectra of the 1:1 complex, as well as variable temperature experiments (*vide infra*). Consistent empirically with intercalation, the phi proton resonances display large upfield chemical shift movements upon binding to d(GTGCAC)$_2$. The magnitude of shifts [phi (1,8), 1.18 ppm; phi (2,7), 1.25 ppm; phi (3,6), 0.55 ppm; and phi (4,5), 0.58 ppm] indicates that all the phi protons are inserted into the aromatic base stack of DNA upon binding. The relative ordering of these chemical shift movements provides a means to estimate the orientation of the phi ligand within the base stack of DNA. The largest shifts are observed for the phi (1,8) and phi (2,7) protons, indicating that these protons are located near the center of the G_3 residue but in a plane above or below where the ring current fields of the aromatic DNA base would be most strong (Giessner-Prettre & Pullman, 1976). Such a model necessarily places the phi (3,6) and phi (4,5) protons at the edge of the base pair, consistent with their smaller upfield shifts.

In contrast to the sharp, well-resolved resonances of the Δ-Rh(en)$_2$phi^{3+}−d(GTGCAC)$_2$ complex, the titration of the oligonucleotide with Λ-Rh(en)$_2$phi^{3+} yields a pronounced broadening of DNA resonances. As illustrated in Figure 3, this broadening occurs at all aromatic and H1′ protons, consistent with the low level of sequence selectivity exhibited in DNA photocleavage studies with Λ-Rh(en)$_2$phi^{3+}. However, the thymine methyl region displays two relatively well-resolved resonances upon addition of Λ-Rh(en)$_2$phi^{3+} (δ =

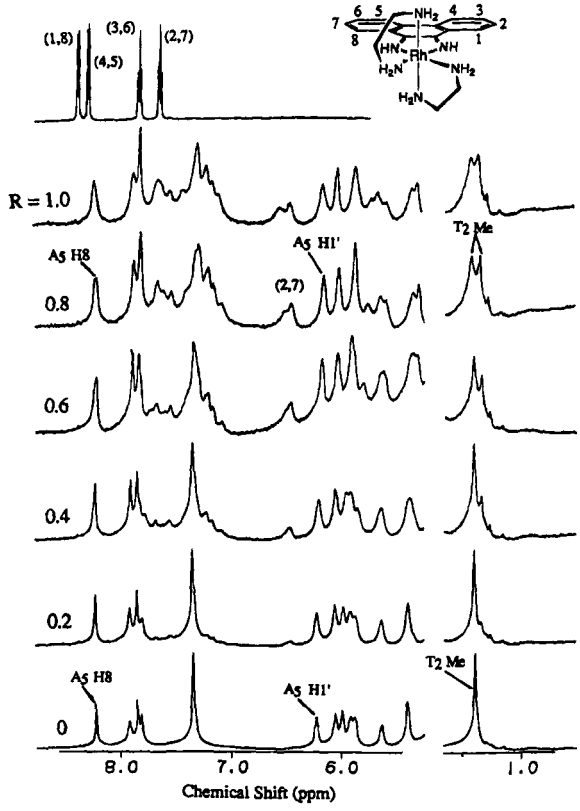

FIGURE 3: ^{1}H NMR titration of d(GTGCAC)$_2$ with Λ-Rh(en)$_2$phi^{3+} at 295 K. 500 MHz ^{1}H NMR spectra are displayed at metal to duplex ratios of (A) 0, (B) 0.2, (C) 0.4, (D) 0.6, (E) 0.8, and (F) 1.0. The spectrum of free Rh(en)$_2$phi^{3+} under identical solution conditions at the top. In contrast to titrations with the Δ-enantiomer, addition of Λ-Rh(en)$_2$phi^{3+} to d(GTGCAC)$_2$ results in broadening of resonances of both the base H8/H6 and sugar H1′ regions. This broadening reflects both the low sequence selectivity of Λ-Rh(en)$_2$phi^{3+} and a slightly faster inherent exchange rate. Importantly, there is a loss of C_2 symmetry in both the metal complex [noted in the phi (2,7) protons at 6.43 and 6.53 ppm] and the T_2 Me resonance.

1.41 and 1.35 ppm). At a stoichiometry of 1 metal per duplex, it appears that the two forms are present in roughly equivalent amounts, although quantitative integration is not possible due to the broad nature of even these resolved resonances. These results indicate that, despite the low overall selectivity of the Λ-enantiomer, there may be a preference in binding of the enantiomer within the T_2G_3 step of the oligomer. With binding to this site, the removal of the C_2 symmetry of the DNA duplex is expected to yield two methyl resonances, one resonance shifted by intercalation of Λ-Rh(en)$_2$phi^{3+} and another resonance very similar to the free oligomer. Further support for this model is evident in spectra of the 1:1 complex at low temperature, 280 and 285 K, where two resonances are similarly observed for the A_5 H8 resonance. A comparable effect would be evident with binding at the G_1T_2 step. Binding in the T_2G_3 site on the oligomer d(GTGCAC)$_2$ is further consistent with photocleavage studies on oligonucleotide and restriction fragment substrates (Shields & Barton, 1995).

Despite the broad nature of the spectra of the 1:1 Λ-Rh(en)$_2$phi^{3+}−d(GTGCAC)$_2$ complex at 295 K, assignments of the chemical shifts of the phi ligand protons were possible using 2D-COSY studies of the 1:1 complex at 285 K. As for the Δ-isomer and consistent with intercalation, the aromatic protons of the phi ligand display strong upfield

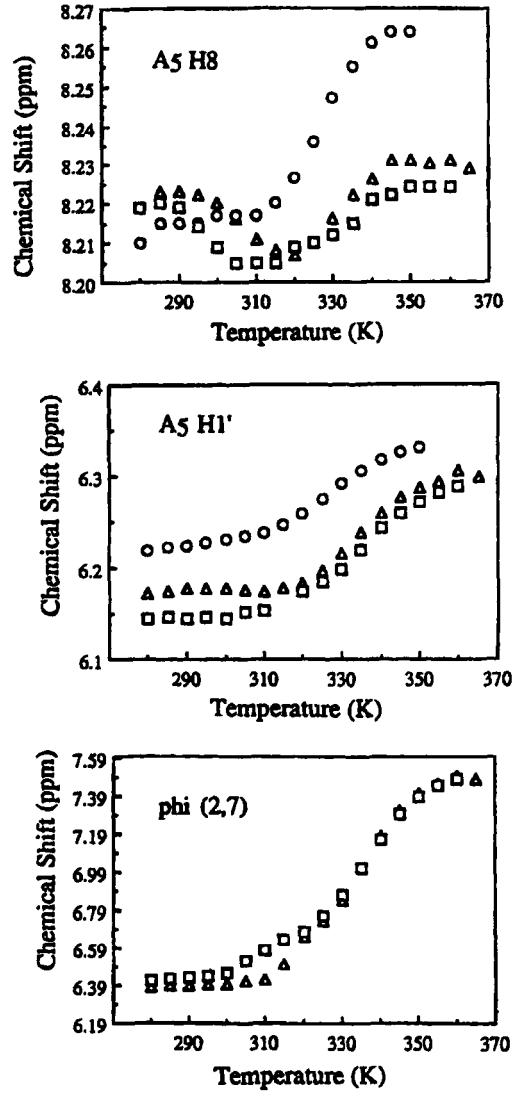

FIGURE 4: Melting curves of the free d(GTGCAC)$_2$ duplex and Λ- and Δ-Rh(en)$_2$phi^{3+}−d(GTGCAC)$_2$ complexes. Spectra were analyzed, and the data are displayed here as plots of chemical shift versus temperature for the A_5 H8 , A_5 H1′, and phi (2,7) resonances in panels A, B, and C, respectively. In all three panels, free duplex protons are indicated with open circles, while protons from Λ- and Δ-Rh(en)$_2$phi^{3+}−d(GTGCAC)$_2$ complexes are shown with open squares and triangles, respectively. Melting points for the complexes may be estimated from the inflection points of these curves. Note that, for both the A_5 H8 and A_5 H1′ protons, the Λ- and Δ-Rh(en)$_2$phi^{3+}−d(GTGCAC)$_2$ complexes are stabilized by 5−10 K relative to the free duplex. Furthermore, the positions of the melting transition of the 1:1 metal−DNA complexes are similar for all three protons shown.

movements in chemical shift upon addition to the oligomer. Despite the differences noted between the general appearance of spectra of Λ- and Δ-Rh(en)$_2$phi^{3+} complexes with d(GTGCAC)$_2$ their apparent binding selectivities, as well as their exchange kinetics, there is a remarkable similarity in the upfield chemical shifts for the two enantiomers bound to the duplex. The results, listed in Table 2, indicate that the two enantiomers intercalate to a common depth into the base stack of DNA. Subtle differences are evident; the greater shift of the 3,6 protons for the Λ-isomer versus the high shift of the 2,7 protons for the Δ-isomer may indicate a deeper fit for the right-handed isomer into the right-handed helix (Barton, 1986). Nonetheless, the stacking of the two isomers seems remarkably close. Therefore, the difference

Table 2: Chemical Shift Movements of Phi Ligand Protons upon Binding to d(GTGCAC)$_2$ at 295 K[a,b]

proton	Rh(en)$_2$phi^{3+} δ	Λ-Rh(en)$_2$phi^{3+}−DNA δ (change)	Δ-Rh(en)$_2$phi^{3+}−DNA δ (change)
1,8	8.37	7.23 (−1.14)	7.18 (−1.19)
4,5	8.28	7.67 (−0.61)	7.70 (−0.58)
3,6	7.81	7.13 (−0.68)	7.27 (−0.54)
2,7	7.63	6.48[c] (−1.15)	6.38 (−1.25)

[a] All data are listed in ppm, referenced to TSP at 295 K. [b] Assignments were based on 2D-NOESY and COSY spectra. [c] This value represents the average of the two phi (2,7) resonances.

in sites selected by Λ- and Δ-Rh(en)$_2$phi^{3+} evident in the spectra must be due largely to the interactions of the ancillary ethylenediamine ligands with DNA.

Importantly, the phi (2,7) protons of the Λ-isomer appear as two broad resonances at 6.53 and 6.43 ppm in Figure 3. While the inequivalence of the phi (2,7) protons may reflect the global loss of C_2 symmetry upon binding of Λ-Rh(en)$_2$phi^{3+} at the T_2G_3 step, another possibility is that the inequivalence reflects canting of the molecule toward one strand of the helix within an intercalation site. This notion is consistent also with the observation that the recognition of 5′-(G)TG-3′ sites by Λ-Rh(en)$_2$phi^{3+} is accompanied by an asymmetrical photocleavage pattern, reflecting a canting of the metal complex within the site (Krotz et al., 1993a,b; Shields & Barton, 1995).

Variable Temperature ^{1}H NMR Experiments. The binding of intercalators to duplex DNA leads to an increase in the duplex melting temperature due to the stabilization of the helix by intercalation (Feigon et al., 1984; Patel & Canuel, 1977; Patel & Shen, 1978; Wilson et al., 1985; Chandrasekaran et al., 1985; Delbarre et al., 1983; Cantor & Schimmel, 1980). A 1D-NMR variable temperature experiment with free d(GTGCAC)$_2$ was conducted as were similar experiments with the 1:1 complexes of Λ- and Δ-Rh(en)$_2$phi^{3+}. As seen in the melting curves for several resonances in Figure 4, a strong melting transition occurs in the free DNA duplex with its center around 330 K. This transition is marked by a strong downfield shifting of the aromatic and H1′ resonances as well as pronounced sharpening of the peaks. With increasing temperature (from 300 to 360 K) the Λ- and Δ-Rh(en)$_2$phi^{3+}−d(GTGCAC)$_2$ complexes also display strong melting transitions, characterized by the sharpening and shifting of the phi ligand protons as well as the DNA aromatic and H1′ resonances. Due to the broad appearance of resonances in the Λ-Rh(en)$_2$phi^{3+}−d(GTGCAC)$_2$ complex, it is not possible to assign completely the aromatic region of the spectra at all temperatures. However, a direct comparison between the Λ- and Δ-Rh(en)$_2$phi^{3+} complexes is possible over the entire temperature range for several DNA resonances, as well as for the phi (2,7) protons. Importantly, the position of the strong melting transition for both 1:1 metal DNA complexes is at 335−340 K. The binding of both enantiomers therefore produces a 5−10° net stabilization of the duplex. This thermodynamic stabilization is expected with intercalation. It appears, furthermore, that both enantiomers stabilize the helix to a similar degree.

It is noteworthy that, in the plots of chemical shift versus temperature shown in Figure 4, the A_5 H8 protons in both 1:1 Rh(en)$_2$phi^{3+}−d(GTGCAC)$_2$ complexes exhibit a premelting transition between 280 and 320 K. This pretransition is characterized by a small upfield movement in chemical shift preceding the larger downfield transition associated with duplex melting. Similar pretransitions are observed in melting curves of several protons in the free DNA (data not shown). This pretransition is typical near DNA ends in the hexamer.

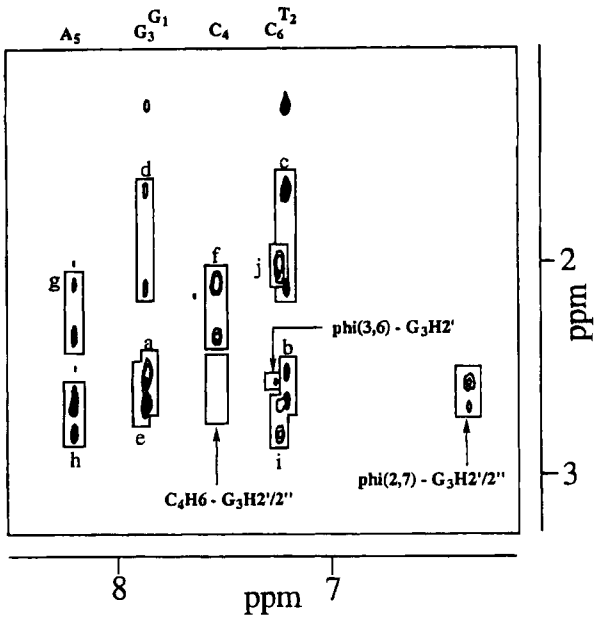

FIGURE 5: Expansion of a 200 ms mixing time 2D-NOESY spectrum at 295 K of the 1:1 Δ-Rh(en)$_2$phi^{3+}−d(GTGCAC)$_2$ complex (0.9 mM in 10 mM phosphate buffer, 20 mM NaCl, pH 7) showing the base H8/H6 to sugar H2′2″ region. The lettered boxes a−j illustrate the sequential path of inter- and intranucleotide NOE cross peaks, starting with the G1 intranucleotide NOE (i.e., G1 H8 to G1 H2′2″). The missing internucleotide connectivity between the G3 H2′2″ and C4 H6 protons is shown with an unlettered box. Intermolecular cross peaks are evident from phi (2,7) to G3 H2′2″ and phi (3,6) to G3 H2′ protons.

The variable temperature experiments also offer an opportunity to estimate the exchange rate for Λ-Rh(en)$_2$phi^{3+} protons with the duplex (Becker, 1980). On the basis of the difference in chemical shift of the A_5 H8 resonances at 280 K, an upper limit of 55 s^{-1} is placed on the exchange rate at the coalescence temperature of 300 K. Similarly, a value of 100 s^{-1} at 310 K may be estimated on the basis of the inequivalence of the phi (2,7) resonances at 290 K.

Another point worthy of note in these studies is that both enantiomers remain associated with the oligomer even at the highest temperatures examined. While the DNA protons in the presence or absence of the metal complex display relatively similar chemical shifts at high temperature, the chemical shifts of both enantiomers of Rh(en)$_2$phi^{3+} are still perturbed relative to the spectrum of free Rh(en)$_2$phi^{3+} at 360 K. This result may reflect the strong electrostatic association of these trications with the hexamer duplex.

2D-NMR Experiments with 1:1 Δ-Rh(en)$_2$phi^{3+}−d(GTGCAC)$_2$. The 1:1 Δ-Rh(en)$_2$phi^{3+}−d(GTGCAC)$_2$ adduct was further examined using 2D-NOESY spectroscopy. As described above, in the NOESY spectrum of free d(GTGCAC)$_2$, an NOE is observed between each base H8 or H6 resonance to its own sugar H2′2″ protons, as well as to the H2′2″ protons of the nucleotide residue in the 5′-direction. However, in the 200 ms NOESY spectrum of Δ-Rh(en)$_2$phi^{3+}−d(GTGCAC)$_2$ (Figure 5), there is a complete absence of internucleotide NOE connectivity between the C_4 H6 and G_3 H2′2″ protons. This selective NOE loss

therefore indicates that the distance between the C_4 H6 proton and the G_3 sugar residue has significantly increased upon binding of Δ-Rh(en)$_2$phi^{3+}. Given the long mixing time (200 ms), such an NOE contact would be expected if the distance between the G_3 and C_4 base residues in the Δ-Rh(en)$_2$phi^{3+}–d(GTGCAC)$_2$ complex were less than ~5 Å. This NOE is also absent in a 300 ms mixing time NOESY experiment (data not shown). Importantly, coincident with this loss of internucleotide connectivity, we observe new NOE cross peaks between the aromatic phi protons and the G_3 H2′2″ protons. Taken together, these observations support the sequence-specific intercalation of Δ-Rh(en)$_2$phi^{3+} between the G_3 and C_4 bases of the oligomer. It is noteworthy that a similar test of loss in NOE connectivity could not be carried out using the H1′ protons because of overlapping resonances.

Given the small number of nonexchangeable protons on Δ-Rh(en)$_2$phi^{3+}, only a few intermolecular NOE's are expected in the 1:1 complex. No intermolecular NOE's are observed between the ancillary ethylenediamine protons and the DNA. This result may indicate dynamic changes in puckering of the chelate ring. Several puckering conformations are evident in crystal structures of the Rh(phi)$^{3+}$ complexes containing aliphatic amines (Schaefer et al., 1992; Krotz et al., 1993a,b). In Figure 5, the only strong intermolecular NOE cross peak observed is from the phi (2,7) to the G_3 H2′2″ protons above and below the intercalation site, and this interaction is marked by a stronger cross peak to the H2″ proton compared to the H2′ proton. There is also a weak cross peak evident between the phi (3,6) and G_3 H2′ protons. A similar weak NOE between the phi (1,8) proton and the G_3 H2′ resonance is observed in a 300 ms mixing time NOESY experiment (data not shown). There are no contacts evident in either 200 or 300 ms NOESY spectra between the phi (4,5) protons and DNA protons, nor would they be expected on the basis of our model. Additionally and not surprisingly, there are no NOE's evident to the A_5 H2 proton, a generally useful marker of minor groove contacts. While these few intermolecular NOE cross peaks do not allow a detailed picture of the intercalation site, they do complement the loss of NOE connectivity between the G_3 and C_4 residues and thus support the intercalation of the phi ligand between the G_3 and C_4 bases of the duplex.

DISCUSSION

The ^{1}H NMR results described here provide a sound structural basis for examining the enantioselectivity in DNA binding of Rh(en)$_2$phi^{3+}. Overall, Λ- and Δ-Rh(en)$_2$phi^{3+} bind to d(GTGCAC)$_2$ in a very similar fashion, characterized as classical intercalation, involving the full insertion of the heterocyclic aromatic phi ligand into the DNA base stack. The phi ligand protons of both enantiomers display similar chemical shift changes upon intercalation. Both enantiomers also stabilize the helix to thermal denaturation. These results therefore indicate an intercalative interaction for both Λ- and Δ-Rh(en)$_2$phi^{3+} bound to the DNA duplex.

The sequence selectivities for the isomers are also reflected in the ^{1}H NMR results. DNA photocleavage results (Krotz et al., 1993a,b; Shields & Barton, 1995) indicate differing sequence selectivities for the two enantiomers. The low level of sequence selectivity displayed by Λ-Rh(en)$_2$phi^{3+} in photocleavage assays is mirrored in the ^{1}H NMR spectra by the pronounced broadening and shifting of d(GTGCAC)$_2$ protons upon binding. Although it appears that the complex binds selectively at the 5′-TG-3′ step of the oligomer, the low overall level of selectivity precludes a firm assignment. Also as predicted by photocleavage studies, Δ-Rh(en)$_2$phi^{3+} binds to d(GTGCAC)$_2$ at the G_3C_4 step and disrupts the internucleotide NOE connectivity between the two bases, consistent with intercalation. Although the data presented here do not allow for the quantitative modeling of the binding site, the combination of the strong upfield chemical shifts of the phi (2,7) and phi (1,8) protons, the loss of internucleotide NOE connectivity, and the discovery of new intermolecular NOE contacts clearly places the Δ-Rh(en)$_2$phi^{3+} deeply within the G_3C_4 intercalation site.

It is useful to revisit the molecular models of Λ- and Δ-Rh(en)$_2$phi^{3+} bound to the DNA duplex developed on the basis of biochemical experiment (Krotz et al., 1993a,b; Shields & Barton, 1995). Figure 6 illustrates models of Δ-Rh(en)$_2$phi^{3+} intercalated within a 5′-GC-3′ step and Λ-Rh(en)$_2$phi^{3+} within a 5′-TA-3′ step. These models, generated on the basis of the DNA site selectivity data (Shields & Barton, 1995), are supported by the NMR data reported here. In these models, the stacking of the phi ligand for both enantiomers is in accordance with the upfield shifts expected on the basis of ring currents generated by intercalative stacking between the base pairs (Giessner-Prettre & Pullman, 1976); the phi (2,7) and phi (1,8) protons are stacked to a significantly greater degree than the phi (3,6) and phi (4,5) protons, which nearly rest in the minor groove of the helix. The phi ligands of both Λ- and Δ-Rh(en)$_2$phi^{3+} are also shown intercalated at a depth similar to that yielded by the energy-minimized structure of Rh(NH$_3$)$_4$phi^{3+}–d(TGGCCA)$_2$ (Collins et al., 1994). ^{1}H NMR studies of Rh(NH$_3$)$_4$phi^{3+} bound to d(TGGCCA)$_2$ show a comparable upfield shift for the phi protons of 1.10, 0.84, 0.60, and 0.59 for the phi (2,7), phi (1,8), phi (3,6), and phi (4,5) protons, respectively. Moreover, a similar stacking is evident in the structure of Δ-α-[Rh-(*R*,*R*)-Me$_2$-(trien)phi]$^{3+}$ intercalatively bound in a DNA decamer, determined using NMR restraints and molecular dynamics (Hudson et al., 1995). It is important to note, however, that the models illustrated here have not been generated using NMR restraints; the data described are insufficient to warrant a detailed structural determination. Nonetheless, the NMR data reported here are fully consistent with biochemical studies on Rh(en)$_2$phi^{3+} isomers (Krotz et al., 1993a; Shields & Barton, 1995) and NMR studies on derivative phi complexes (Collins et al., 1994; Hudson et al., 1995).

The NMR data primarily indicate the deep intercalation of the phi ligand, and these models illustrate that a full intercalation of the phi ideally locates the ethylenediamine ligands to engage in hydrogen bonding and van der Waals contacts with the DNA major groove. The full intercalation of the phi ligand does not create steric clashes between ancillary ligands and DNA, given the small expanse of the en ligand, but in fact positions the axial amines and Λ-methylene groups in ideal positions for hydrogen bonding and van der Waals contacts with the bases, respectively. It is noteworthy that the NMR data are insufficient to speak to the details of the orientation of the phi ligand within the base stack. In fact, evidence for an association from the major groove for these enantiomers rests upon the sensitive dependence of recognition by both isomers to base modifications in the major groove (NMR experiments on the

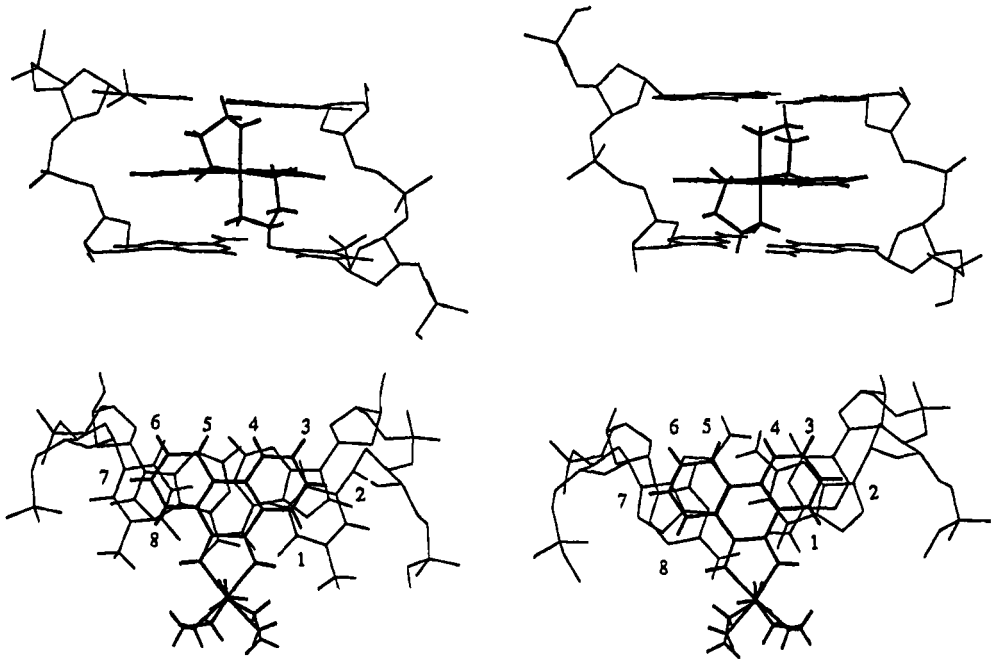

FIGURE 6: Molecular models of Λ-$Rh(en)_2phi^{3+}$ intercalated into 5′-TA-3′ (left) and Δ-$Rh(en)_2phi^{3+}$ intercalated into 5′-GC-3′ (right). Shown are views down the helical axis (below), as well as perpendicular to the axis (top). These models, generated on the basis of biochemical results, are consistent with the NMR experiments described here. In order to show the depth of intercalation, the phi ligand protons have been numbered. The intercalation of both Λ- and Δ-$Rh(en)_2phi^{3+}$ is illustrated intercalated to a similar depth, based upon the chemical shift data. Importantly, when the enantiomers of $Rh(en)_2phi^{3+}$ are intercalated as shown, the ancillary ethylenediamine ligands are ideally located to engage in hydrogen bonding and van der Waals contacts.

derivative Δ-α-$[RhMe_2(trien)phi]^{3+}$ also show direct intermolecular methyl−methyl contacts in the major groove). Nonetheless, with these models, it is evident that the relatively sequence-neutral intercalative interaction is complemented by noncovalent contacts by the ancillary ligands, which appear to determine the site selectivity of the metal complex.

While the photocleavage of DNA by $Rh(phen)_2phi^{3+}$ produces cleavage at only the 5′-residue of an intercalation site, it has been observed that photocleavage by the smaller $Rh(en)_2phi^{3+}$ complexes is often characterized by cleavage at both 5′- and 3′-residues of the intercalation site (Shields & Barton, 1995). The ^1H NMR results described here may also shed light on this difference in photocleavage for $Rh(N_4)phi^{3+}$ [$N_4 = (NH_3)_4$, $(en)_2$, or cyclen] complexes (Shields & Barton, 1995). The upfield shifts for the DNA-bound aliphatic amine complexes (0.59−1.1 ppm) compared to $Rh(phen)_2phi^{3+}$ indicate a deeper intercalation for the aliphatic amine complexes; upfield shifts are in the range of 0.58−0.88 for Δ-$Rh(phen)_2phi^{3+}$ bound to DNA (David & Barton, 1993). This deeper intercalation of the smaller $Rh(en)_2phi^{3+}$ allows closer access of the phi ligand to the 3′-sugar of the intercalation site. Interestingly, molecular modeling predicts that the H2′ proton is the most directly accessible proton of the 3′-sugar. Although hydrogen atom abstraction is disfavored energetically by 2 kcal/mol relative to the H3′ position (Miaskiewicz & Osman, 1994), the effective reactivity would be expected to be highly controlled by accessibility. Furthermore, initial abstraction of the H2′ atom would likely be followed by fast H atom migration from the *cis*-positioned H3′ (not the *trans*-oriented H1′), and thus, the overall chemistry would appear to occur at the C3′ position of the sugar. Such a model might be tested through substitution of ribonucleotides into an otherwise DNA duplex, since the C2′-radical would be stabilized by substitution with the heteroatom.

The NMR evidence presented here allows also interesting comparisons to be drawn between the nonspecific classical intercalator ethidium bromide and the nonclassical metallointercalators $Rh(en)_2phi^{3+}$ and $Rh(NH_3)_4phi^{3+}$ (Collins et al., 1994). With all these intercalators, the full insertion of the aromatic moiety leads to a high overall affinity for DNA. However, the relatively sequence-neutral intercalative binding event may be improved through the unique potential of octahedral metal complexes to utilize their ancillary ligands for site discrimination. Although the level of sequence selectivity in Δ-$Rh(en)_2phi^{3+}$ and $Rh(NH_3)_4phi^{3+}$ is not high, these complexes are significantly more sequence selective compared to ethidium bromide. This effect is a result of the hydrogen bonding and van der Waals contacts between the ancillary ethylenediamine ligands and the functionalities of the DNA major groove.

The structural data for $Rh(en)_2phi^{3+}$ and $Rh(NH_3)_4phi^{3+}$ may also be compared to that obtained for the shape-selective complex Δ-$Rh(phen)_2phi^{3+}$ (David & Barton, 1993). In contrast to the enantioselectivity of $Rh(en)_2phi^{3+}$, which is based upon positive hydrogen bonding and van der Waals contacts, the sequence selectivity of $Rh(phen)_2phi^{3+}$ is primarily due to steric interactions (Campisi et al., 1994). Again, the intercalation of the phi ligand in $Rh(phen)_2phi^{3+}$ is marked by a substantial upfield movement in the chemical shift of the phi ligand protons: phi (1,8), 0.58 ppm; phi (2,7), 0.83 ppm; phi (3,6), 0.88 ppm; phi (4,5), 0.73 ppm. However, the distribution of the chemical shift changes, largest at the phi (3,6) positions, supports a model where for $Rh(phen)_2phi^{3+}$ the phi ligand is not as deeply intercalated into the DNA double helix as for $Rh(en)_2phi^{3+}$. Molecular modeling indicates that the phi ligand in $Rh(phen)_2phi^{3+}$ may

not be completely inserted into the base stack without the propeller twisting of the bases because of steric clashes with the ancillary phenanthrolines. This intercalation of the phi ligand in $Rh(phen)_2phi^{3+}$, then, positions the ancillary phenanthrolines so that they may discriminate between sites based upon shape, and $Rh(phen)_2phi^{3+}$ binds to sites that are open in the major groove (Pyle et al., 1990; Sitlani et al., 1992; Campisi et al., 1994). $Rh(en)_2phi^{3+}$ appears, in contrast, not to utilize shape selection as an element of site-recognition.

CONCLUSIONS

This work provides structural evidence that both Λ- and Δ-$Rh(en)_2phi^{3+}$ bind to DNA by the full intercalation of the heterocyclic aromatic phi ligand between the base pairs of DNA. Variable temperature studies also show a common helix stabilization by the two isomers. The deep intercalation of the phi ligand does not cause clashes between the DNA and the small ancillary ligands but, rather, ideally positions the molecule to engage in hydrogen bonding and van der Waals contacts with base functionalities in the major groove of DNA. In molecular models generated on the basis of biochemical studies and supported by the NMR results, the axial amines of Δ-$Rh(en)_2phi^{3+}$ are well positioned to make hydrogen bonding contacts to the guanine O6 atoms above and below the intercalation site. Although NMR results for Λ-$Rh(en)_2phi^{3+}$ support intercalation, little selectivity is evident. Both $Rh(en)_2phi^{3+}$ isomers bind the duplex similarly, by intercalation, but differently because of the different noncovalent interactions available for the ancillary ligands. Exploiting the intercalation of the $Rh(phi)^{3+}$ moiety as an anchor in the major groove of DNA therefore points to a general strategy for the design of sequence-specific DNA-binding molecules.

REFERENCES

Barton, J. K. (1986) *Science 233*, 727.

Becker, E. D. (1980) *High Resolution NMR: Theory and Chemical Applications*, 2nd ed., Academic Press, New York.

Campisi, D., Morii, T., & Barton J. K. (1994) *Biochemistry 33*, 4130.

Cantor, C. R., & Schimmel, P. R. (1980) *Biophysical Chemistry*, Part III, W. H. Freeman and Co., San Francisco.

Chandrasekaran, S., Jones, R. L., & Wilson, W. D. (1985) *Biopolymers 24*, 1941.

Collins, J. G., Shields, T. P., & Barton, J. K. (1994) *J. Am. Chem Soc. 116*, 9840.

David, S. D., & Barton, J. K. (1993) *J. Am. Chem. Soc. 115*, 2984.

Delbarre, A., Gourevitch, M. I., Gaugain, B., Le Pecq, J. B., & Roques, B. P. (1983) *Nucleic Acids Res. 11*, 4467.

Dupureur, C. M., & Barton, J. K. (1995) The Assembly of Transition Metal Complexes for Site-specific Recognition of Nucleic Acids, in *Comprehensive Supramolecular Chemistry* (Lehn, J.-M., Ed.) Vol. 5, Pergamon Press, New York (in press).

Eriksson, M., Leijon, M., Hirot, C., & Norden, B. (1992) *J. Am. Chem. Soc. 114*, 4933.

Feigon, J., Denny, W. A.., Leupin, W., & Kearns, D. R. (1984) *J. Med. Chem.*, 450.

Giessner-Prettre, C., & Pullman, B. (1976) *Biochem. Biophys. Res. Commun. 70*, 578.

Hudson, B. P., Dupureur, C. M., & Barton, J. K. (1995) *J. Am. Chem. Soc. 117*, 9379.

Krotz, A. H., Kuo, L. Y., & Barton, J. K. (1993a) *Inorg. Chem 32*, 5963.

Krotz, A. H., Kuo, L. Y., Shields, T. P., & Barton, J. K. (1993b) *J. Am. Chem Soc. 115*, 3877.

Liu, X. L., Chen, H., & Patel, D. J. (1991) *J. Biomol. NMR 1*, 323.

Marion, D., & Wuthrich, K. (1983) *Biochem. Biophys. Res. Commun. 113*, 967.

Miaskiewicz, C., & Osman, R. (1994) *J. Am. Chem. Soc. 116*, 232–238.

Patel, D. J., & Canuel, L. L. (1977) *Biopolymers 16*, 857.

Patel, D. J., & Shen, C. (1978) *Proc. Natl. Acad. Sci. U.S.A. 75*, 2553.

Patel, D. J., & Shapiro, L. (1986a) *Biopolymers 25*, 707.

Patel, D. J., & Shapiro, L. (1986b) *J. Biol. Chem. 261*, 1230.

Patel, D. J., Shapiro, L., & Hare, D. (1986) *J. Biol. Chem. 261*, 1223.

Pyle, A. M., Morii, T., & Barton, J. K. (1990) *J. Am. Chem. Soc. 112*, 9432–9434.

Rehmann, J. P., & Barton, J. K. (1990a) *Biochemistry 29*, 1701.

Rehmann, J. P., & Barton, J. K. (1990b) *Biochemistry 29*, 1710.

Schaefer, W. P., Krotz, A. H., Kuo, L. Y., Shields, T. P., & Barton, J. K. (1992) *Acta Crystallogr. C48*, 2071.

Shields, T. P., & Barton, J. K. (1995) *Biochemistry 34*, 15037–15048.

Sitlani, A., Long, E. C., Pyle, A. M., & Barton, J. K. (1992) *J. Am. Chem. Soc. 114*, 2303.

Wang, A. H. J., Nathans, J., van der Marel, G., van Boom, J. H., & Rich, A. (1978) *Nature 276*, 471.

Wilson, W. D., Krishnamoorthy, C. R., Wang, Y. H., & Smith, J. C. (1985) *Biopolymers 24*, 1941.

Wuthrich, K. (1986) *NMR of Proteins and Nucleic Acids*, Wiley, New York.

BI951329D